Mini Review

Recent Advances in LiFePO₄ Cathode Materials for Lithium-Ion Batteries. First-Principles Research

Qun-fang Zhao[1,2,3,&], Shu-qiong Zhang[1,2,3,&], Min-yi Hu[1,2,3], Chang Wang[1,2,3], Guang-hui Jiang[1,2,3,]*

[1] Advanced Batteries and Materials Engineering Research Center, Guizhou Light Industry Technical College, Guiyang 550025, China;
[2] Graphene Materials Engineering Research Center of Guizhou Colleges and Universities, Guiyang 550025, China;
[3] Provincial Collaborative Innovation Center of Used Power Batteries Recycling, Guiyang 550025, China;
& These authors contributed equally to this work and should be considered co-first authors
[*]E-mail: jianggh88@foxmail.com

Lithium-ion batteries (LIBs) are the dominant battery technologies from portable electronics to electronic vehicles due to their high energy density and excellent cycling performance. The discovered LiFePO₄ cathode with good cycling stability, low price and excellent safety is one of the most attractive cathode materials for LIBs. However, several crucial challenges including poor ionic and electronic conductivity and low Li⁺ diffusion impede its high-rate application. To improve these troublesome issues, many investigations have been performed, and the electrochemical performance of LiFePO₄ has been enhanced. However, the modified origins of the electronic structure and ionic dynamic properties of LiFePO₄ cathodes are still being explored. Computational research provides a better understanding of the above improvements to a significant extent. In this review, recent achievements in first-principles studies of LiFePO₄ cathode materials are discussed, including structure, electronic properties, Li-ion transport characteristics, mechanical stability and thermodynamic properties.

1. INTRODUCTION

With the emergence of the oil crisis and finite resources of the earth, the increasing demand for environmental protection and the continuous development of electronic technology have facilitated the research and progress of lithium-ion batteries (LIBs). LIBs were successfully commercialized by SONY in 1991 [1]. LIBs are also considered to be one of the most promising batteries owing to their high power density, long cycle life and environmental friendliness. The cathode material is the most crucial

Int. J. Electrochem. Sci., 16 **(2021)** Article Number: 211226

2

component of lithium-ion batteries. Therefore, tremendous efforts have been dedicated to the development of cathode materials. The cathode materials of LIBs are usually intercalation compounds, including layered $LiMO_2$ (M=Co, Ni, Mn), $LiNi_{1-x-y}Co_xMn_y$, spinel $LiMn_2O_4$ and olivine $LiFePO_4$ materials [2-6]. Among them, olivine-structured $LiFePO_4$ was proposed in 1997 by Padhi [7] with excellent cycling stability, low cost and good safety. Nevertheless, the poor ionic and electronic conductivity and low Li^+ diffusion has hindered its further application [8]. Morphology control, particle size reduction, surface coatings and cation or anion doping have been applied to improve its properties [9-14]. Furthermore, it is significant to explicitly understand the microscopic origins of these improvements.

First-principles calculations were used to identify cathode materials for LIBs in 1997 [15]. Hence, theoretical studies of $LiFePO_4$ play a guiding role in improving its performance. Diverse properties, such as structure, conduction behavior, Li-ion diffusion, mechanical stability and thermal performance, can be assessed by computational methods [16-20]. Recent reviews have mainly focused on experimental studies of $LiFePO_4$, but there have been few reviews using first-principles calculations. As a consequence, here, first-principles studies on the structure, electronic properties, Li-ion transport characteristics, mechanical stability and thermodynamic properties of $LiFePO_4$ are discussed.

2. PROPERTIES OF LiFePO4

2.1 Structure of LiFePO4

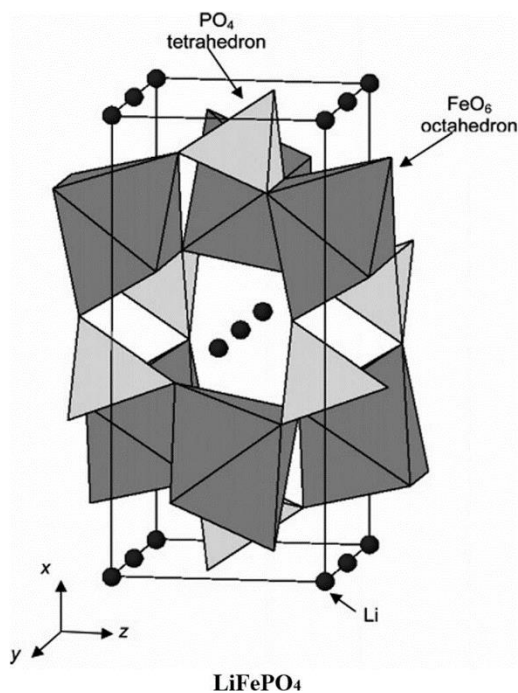The olivine-type $LiFePO_4$ has an orthorhombic crystal structure with a Pnma space group.

Figure 1. The olivine structure of $LiFePO_4$ [21]

Int. J. Electrochem. Sci., 16 **(2021)** Article Number: 211226

3

The unit cell contains four $LiFePO_4$ formula units, where Li (M1) and Fe (M2) are located in octahedral positions, forming octahedrons with O. P is located in a twisted hexagonal densely packed tetrahedron position, forming a tetrahedron with O. The experimental and calculated lattice parameters are listed in Table 1. It is found that the density functional theory (DFT)+U within generalized gradient approximation (GGA)+U is in good accordance with the experimental lattice parameters. $LiFePO_4$ delivers excellent lattice stability because the oxygen atoms are firmly bound to the iron and phosphorus atoms, leading to superior cycling performance and high safety. However, the strong oxygen covalent bonds result in low electron and ionic conductivity.

Table 1. Comparison of the experimental and calculated lattice parameters of $LiFePO_4$

	a [Å]	b [Å]	c [Å]
Expt. [22]	10.3208	6.0046	4.6854
Expt. [23]	10.3312	6.0109	4.6959
Cal. [24]	10.4256	6.0579	4.7437
Cal. [25]	10.427	6.057	4.743

2.2 Electronic property

2.2.1 Magnetic properties

The magnetic properties of $LiFePO_4$ may affect the structural performance and electronic transport mechanisms, which deserves to be explored.
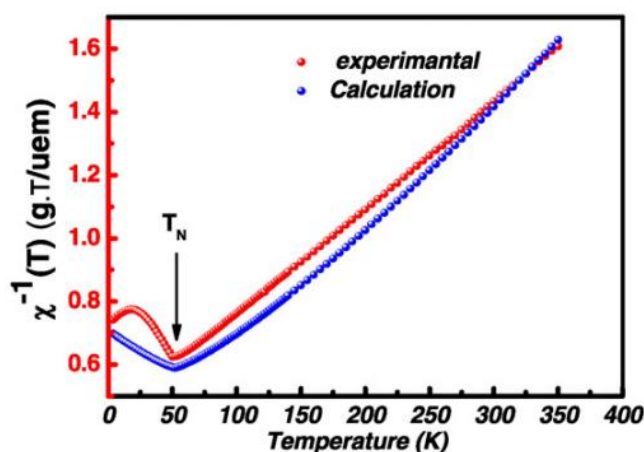

Figure 2. Predicted inverse magnetic susceptibility χ^{-1} (T) compared to experimental data [28]

The low-temperature magnetic ordering, isomer shift and quadrupole splitting in $LiFePO_4$ were evaluated by Mössbauer spectroscopy and first-principles calculations [26-27]. A DFT-based approach was used to investigate the magnetic order and hyperfine interactions, corresponding to the results of

Mössbauer spectroscopy. This confirms that both the Fermi contact term and orbital magnetic moments of Fe ions are dedicated markedly to the hyperfine field.

Masrour et al. [28] calculated the magnetic moments carried by Fe atoms via DFT and the full potential linearized augmented plane wave (FLAPW) method, considering appropriate polarized spin and spin-orbit coupling as well as the antiferromagnetic state. As shown in Fig. 2, the computed inverse magnetic susceptibility is consistent with the experimental findings.

2.2.2 Electronic structure

In solid-state physics, energy band theory describes the motion of electrons in solid materials. Some basic properties of materials are related to their electronic structures, including energy band structure, density of state (DOS), and partial density of states (PDOS). Therefore, electronic structures can be utilized to elaborate and predict these fundamental characteristics. In addition, some performance characteristics can be modulated through electronic structures.

Energy band theory is an approximate single-electron theory. At present, DFT is the most accurate theory for solving single-electron problems. All calculations are generally performed via the Vienna ab initio simulation package (VASP) code [29] or Cambridge serial total energy package (CASTEP) program [30]. The exchange-correlation functional is a GGA [31] and local density approximation (LDA) [32], which is used to precisely calculate the electronic structures of transition metal materials, ignoring the Coulomb repulsion between electrons. As a result, the effective Hubbard-U parameter is set to improve the depiction of the Fe-3d states [33]. For most of the calculations, U is often 4.3, 4.7 or 5.3 eV [34-36].

A narrow bandgap can diminish the transfer barrier of electrons, contributing to the higher electrical conductivity of a material. The calculated bandgap is listed in Table 2. The bandgap ranges from 0.18 eV to 3.74 eV owing to diverse calculation techniques [37-40]. Focusing on the relative values is reasonable. Furthermore, the reduced bandgap of doped $LiFePO_4$ demonstrates that doping is a meaningful modification to enhance the conductivity of $LiFePO_4$ materials.

Table 2. The calculated bandgap of pure and doped $LiFePO_4$

	Calculated bandgap (eV)	method	Ref.
$LiFePO_4$	0.768	DFT	[37]
	3.74	GGA+U	[19]
	3.58	GGA+U	[25]
Sn^{2+} doped	2.96	GGA+U	[19]
N doped	0.65	GGA+U	[25]
Mn^{2+} doped	0.529	GGA	[20]
Al^{3+} doped	0.76	GGA	[20]
$Li_{0.995}K_{0.005}FePO_4$	0.714	GGA+U	[38]
$LiFe_{0.98}V_{0.02}PO_4$	0.633	GGA+U	[22]
$Na_{1/8}Li_{1-1/8}FePO_4$	0.58	GGA	[39]
$LiFe_{1-3/12}Mo_{1/12}PO_4$	0.18	GGA	[40]

The DOS is also beneficial for understanding changes in electronic structure, and the PDOS can assign the contribution of an atom to each band of a given atomic orbital. Ouyang et al. [41] compared the PDOS of pure and Na-doped $LiFePO_4$. This proved that the energy levels at the Fermi level are essentially contributed by Fe-3d in the lattice, as observed from DOS and PDOS by Chen's team [38]. For the cation doped at the Fe site in $LiFePO_4$, our previous research [22] showed that both Fe-3d and V-3d contributed to the electronic states around the Fermi level (Fig. 3). The above findings show that first-principles calculations help to illustrate the conductive and doping behavior of $LiFePO_4$.
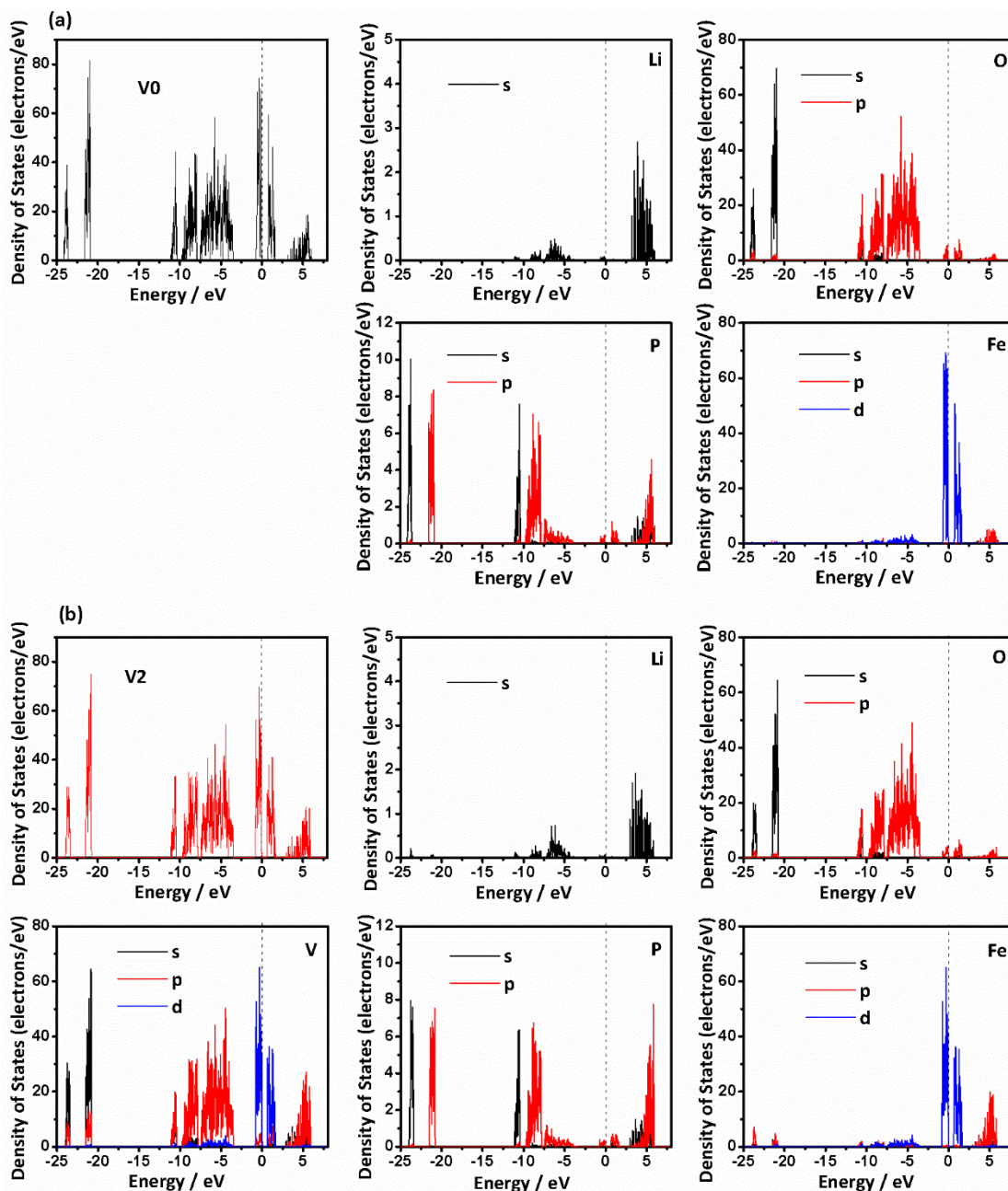

Figure 3. DOS and PDOS for (a) V0 and (b) V2 [22]

2.3 The Li-ion transport characteristic

Both theoretical and experimental findings indicate that Li ions diffuse along a (010) one-dimensional pathway. The slow diffusion coefficient of Li^+ ions (D, 10^{-13}-10^{-14} $cm^2 \cdot s$) in $LiFePO_4$ limits its rate capability, which is related to grain boundaries. Consequently, it is vital to comprehend the improved Li diffusion kinetics in $LiFePO_4$ cathode materials. D can be evaluated by using experiments and theoretical calculations. Although the total D can be measured experimentally from electrochemical impedance spectroscopy (EIS) measurements or the galvanostatic intermittent titration technique (GITT), the computational methods particularly explain the Li-ion diffusion mechanism. The calculations of Li-ion diffusion include nudged elastic band (NEB), Monte Carlo (MC) simulations and molecular dynamics (MD) simulations [42-43].

The NEB method is a way of finding the saddle points and minimum energy pathway for given reactants and products. The diffusion path, diffusion barrier and transition state can be calculated by this method. The MC method can simulate tremendous systems and the states of microscopic particles for materials through random sampling without complex molecular dynamics calculations. This method can establish the relationship between the state of elementary particles and the macroscopic properties of materials, which is an important means to study the characteristics of materials and the nature of their influencing factors. For kinetic problems, the time scale of MC is much larger than that of the molecular dynamics method, so slower kinetic problems can be studied. The MD simulation is a deterministic method to calculate the equilibrium and transfer properties of classical multibody systems. In 1985, R. Car and M. Parrinello first proposed a "unified approach for molecular dynamics and density functional theory" [44].

Xu et al. [45] calculated the minimum energy pathway and diffusion activation energy along a one-dimensional channel for sulfur surface-modified $LiFePO_4$ from first-principles calculations with NEB. The reduced activation energy (approximately 0.18 eV) and surface diffusion coefficient (approximately 10^{-11} cm^2 s) of S-$LiFePO_4$ (010) indicate that the ionic conductivity could be enhanced significantly. Yang et al. [46] studied Li-ion diffusion behavior in $LiFePO_4$ using ab initio MD with spin polarized GGA+U. Li migration (Fig. 4) down a "zigzag" (010) one-dimensional pathway and a (010) channel with the assistance of Li-Fe antisites was observed for the first time. Many experiments have been carried out to investigate the effect of doping on $LiFePO_4$ performance [47-48]. However, the microscopic doping mechanism still needs to be further investigated. The effect of Cr-doped $LiFePO_4$ on Li-ion diffusion was explored by means of first-principles and MC simulations [49]. In this study, the decreased capacity was ascribed to impeded Li migration along the one-dimensional diffusion pathway by Cr doping at the Li site, in accordance with experimental findings [50].
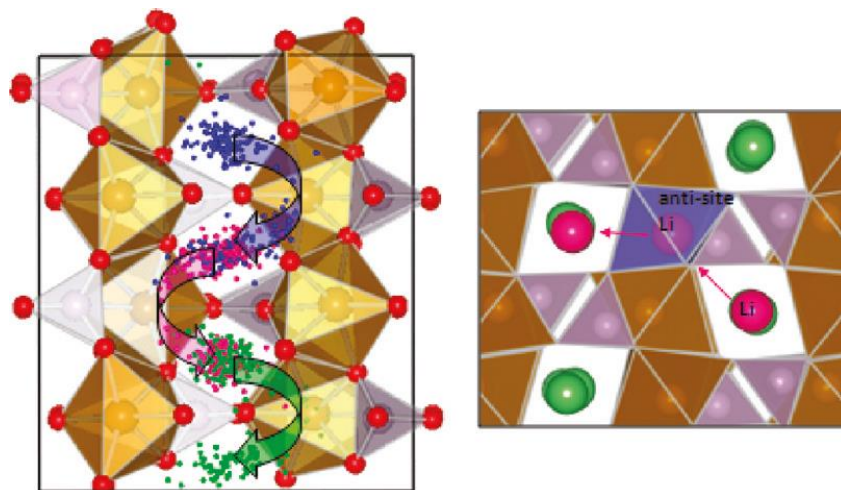
Figure 4. The zigzag diffusion pathway and the second diffusion mechanism involving the formation of Li-Fe antisites [46]

2.4 Mechanical stability

It is urgent to better understand the structural stability of cathode materials because the mechanical stability is closely related to the electrochemical properties of materials during Li intercalation and deintercalation, especially the cyclic performance. Moreover, the mechanical instability generated by phase transition may result in recession of the batteries. The elastic properties are used to characterize the mechanical stability of materials, as well as the Debye temperature (T_D) [51]. As a consequence, the elastic stiffness (C_{ij}) and compliance coefficient (S_{ij}) are usually calculated to describe the elastic properties of materials.

The C_{ij} and T_D were calculated to investigate the mechanical stability of $LiFePO_4$ after doping with Mn, Co, Nb and Mo by means of CASTEP in the DFT framework [52]. In comparison with Nb, the calculation results for the Debye temperature reflected the improved mechanical stability of cathode materials doped with Mn, Co and Mo. In addition, the computational stiffness C_{ij} indicated that doping was feasible and enhanced the stability of the materials. $LiFePO_4$ was more easily affected by shear deformation, which was also observed in another study [53]. The above findings would play a better guiding role in experimental research with doping.

2.5 Thermodynamic properties

$LiFePO_4$ possesses eminent thermal stability. However, the electrochemical performance and safety of $LiFePO_4$ are particularly susceptible to thermodynamic properties during the charge and discharge process. It is necessary to study the thermodynamic properties of $LiFePO_4$, such as entropy, enthalpy and Gibbs energy. The thermodynamic properties of the system are described on the basis of phonons, which are energy quanta of lattice vibrations. The phonon predictions of first principles could confirm the thermodynamic properties at finite temperature [54].

Wang et al. [37] calculated the entropy, enthalpy and Gibbs free energy of LiFePO$_4$ at 1 atmospheric pressure from 100 to 1000 K relying on first-principles DFT. These authors identified that the entropy, enthalpy and Gibbs free energy of LiFePO$_4$ abide by thermodynamic law. In addition, the thermal stabilities of LiFePO$_4$ and other cathode materials (Li$_2$MnO$_4$, LiNiO$_2$, LiCoO$_2$) have been compared by first-principles calculations [53]. Their Gibbs formation energies from oxides were -287.51, −81.87, −48.76 and −133.54 kJ mol^{-1}, which demonstrated that LiFePO$_4$ was more thermodynamically stable.

3. CONCLUSIONS

Among all the candidate cathode materials for LIBs, LiFePO$_4$ is still the dominant cathode material in electric vehicles and portable electronic equipment because of its high safety, excellent cycling stability and low raw material cost. Nevertheless, LiFePO$_4$ demonstrates low ionic conductivity and sluggish Li$^+$ diffusion. In this case, tremendous attention, such as doping, surface coating and particle size reduction methods, has been given to modifying these properties. However, the microscopic origins of the electronic structure and ionic dynamic properties of modified LiFePO$_4$ cathode materials are still ambiguous. First-principles calculations provide a visualization from microscopic to macroscopic scales. In this paper, we briefly outline the recent first-principles research development of the structure, electronic properties, Li-ion transport characteristics, mechanical stability and thermodynamic properties of LiFePO$_4$ cathode materials for LIBs via first-principles studies. With the increasing performance requirements of LiFePO$_4$ cathode materials, it is necessary to explore LiFePO$_4$ in depth. First-principles calculations are a bridge that connects theory and experiment. As a result, the combination of computational and experimental studies will make the research and development of LiFePO$_4$ cathode materials more directional and forward-looking, contributing to greatly improving the research efficiency and wide practical applications.

References

1. C. Y. Xiong, F.C. Liu, J.J. Gao, X. Jiang, *ACS Omega*, 5 (2020) 30356.
2. W. Li, A. Garg, M.L.P. Le, C. Ruhatiya, L. Gao, V. M. Tran, *Electrochim. Acta*, 330 (2019) 135314.
3. M. Kim, J. Zhu, L.Z. Li, C.M. Wang, G. Chen, *ACS Appl. Energy Mater.*, 12 (2020) 12238.
4. Y. Wang, Q.H. Zhang, Z.C. Xue, L.F. Yang, J.Y. Wang, F.Q. Meng, Q.H. Li, H.Y. Pan, J.N. Zhang, Z. Jiang, W.L. Yang, X.Q. Yu, L. Gu, H. Li, *Adv. Energy Mater.*, 10 (2020) 2001413.
5. R.E. Warburton, M.J. Young, S. Letourneau, J.W. Elam, J. Greeley, *Chem. Mater.*, 32 (2020) 1794.
6. S. Ahmed, M. Bianchini, A.j Pokle, M.S. Munde, P.l Hartmann, T. Brezesinski, A. Beyer, J. Janek, K. Volz, *Adv. Energy Mater.*, 10 (2020) 2001026.
7. A. K. Padhi, K. S. Nanjundaswamy, J. B. Goodenough, *J. Electrochem. Soc.*, 144 (1997) 1188.
8. F. Ruiz-Jorge, A. Benítez, S. Fernández-García, J. Sánchez-Oneto, J. R. Portela, *Ind. Eng. Chem.*

Res., 59 (2020) 9318.
9. M. A.M.M.Alsamet, E. Burgaz, *Electrochim. Acta*, 367 (2021) 137530.
10. S.J. Sun, Q.L. An, Z.Q. Tian, X.Y. Zhao, X. Shen, *Energy Fuels*, 34 (2020) 11597.
11. Y. Xi, Y. Lu, *Industrial & Engineering Chemistry Research*, 59 (2020) 13549.
12. X.M. Cui, D.W. Yi, N.L. Li, L. Zhang, X.F. Zhang, D. Yang, *Energy Fuels*, 34 (2020) 7600.
13. Y. Liu, Y.J. Gu, G.Y. Luo, Z.L. Chen, F.Z. Wu, X.Y. Dai, Y. Mai and J.Q. Li, *Ceram. Int.*, 46 (2020) 14857.
14. C.Z. Li, H.Y. Yuan, Z. Yang, *Solid State Ionics*, 352 (2020) 115366.
15. G. Ceder, Y.M. Chiang, D. R. Sadoway, M. K. Aydinol, Y.I. Jang, B. Huang, *Nature*, 392 (1998) 694.
16. J. Kuriplach, A. Pulkkinen, B. Barbiellini, *Condens. Matter*, 4 (2019) 80.
17. S. Kobayashi, A. Kuwabara, C.A.J. Fisher, Y. Ikuhara, *ACS Appl. Energy Mater.*, 3 (2020) 8009.
18. H. Wang, N. Zhao, C. Shi, L. Ma, F. He, C. He, J. Li and E. Liu, *Electrochim. Acta*, 247, 1030 (2017).
19. L. Hou, G. Tao, *Phys. Status Solidi B*, 254 (2017) 1700041.
20. H. L. Zhang, Y. Gong, S. Yang, J. Li, K. Du, J. Li, *Int. J. Electrochem. Sci.*, 13 (2018) 10427.
21. H.H. Zhang, Z.G. Zou, S.C. Zhang, J. Liu, S.L. Zhong, *Int. J. Electrochem. Sci.*, 15 (2020) 12041.
22. Q.F. Zhao, S.Q. Zhang, C. Wang, G.H. Jiang, M.Y. Hu, Z.Y. Chen and Q.S. Ouyang, *Int. J. Electrochem. Sci.*, 16 (2021) 21053.
23. Y. Zhang, J.A. Alarco, J.Y. Nerkar, A.S. Best, G.A. Snook, P.C. Talbot, B. C. C. Cowie, *ACS Appl. Energy Mater.*, 3 (2020) 9158.
24. G. Xu, K. Zhong, Y. Yang, J.M. Zhang, Z. Huang, *Solid State Ionics*, 338 (2019) 25.
25. G. Xu, K. Zhong, J.M. Zhang, Z. Huang, *Solid State Ionics*, 281 (2015) 1.
26. T. Kmjeˇ, J. Kohout, M. Dopita, M. Veverka, J. Kuriplach, *Condens. Matter*, 4 (2019) 86.
27. M. E. Khalifi, P.E. Lippens, *J. Phys. Chem. C*, 120 (2016) 28375.
28. R. Masrour, E. K. Hlil, S. Obbade, C. Rossignol, *Solid State Ionics*, 289 (2016) 214.
29. S. Kim, V.I. Hegde, Z.P. Yao, Z. Lu, M. Amsler, J.G.g He, S.Q. Hao, J.R. Croy, E. Lee, M.M. Thackeray, C. Wolverton, *ACS Appl. Mater. Inter.*, 10 (2018) 13479.
30. Y. Qiang, L. Zhang, S. Shao, J. Li, *Int. J. Energ. Res.*, 45 (2021) 6426.
31. J.j. Miao, C.C. Chai, W. Zhang, Y.X. Song, Y. Yang, *Materials*, 13 (2020) 686.
32. A. Jena, B. R. K. Nanda, *Sci. Rep.,* 6 (2016) 19573.
33. R.C. Xiao, J. Xie, T. Luo, L. Huang, Y. Zhou, D.M. Yu, C.G. Chen, Y. Liu, *J. Phys. Chem. C*, 122 (2018) 1513.
34. G. K.P. Dathar, D. Sheppard, K.J. Stevenson, G. Henkelman, *Chem. Mater.*, 23 (2011) 4032.
35. W. T. Geng, *J. Phys. Chem. C*, 116 (2012) 17650.
36. K. Hoang, M. Johannes, *Chem. Mater.*, 23 (2011) 3003.
37. S. Z. Wang, G. Zhang, J. L. Gao, J. Wang, Y. Y. Wang, C. J. Nan, D. Y. Huang, L. L. Chen, J. F. Song, P. H. Luo, International Workshop on Materials, Chemistry and Engineering, (2018) 133.
38. Z.Y. Chen, Z. Zhang, Q.F. Zhao, J.F. Duan, H.L. Zhu, *J. Nanosci. Nanotechnol.,* 18 (2018) 1.
39. J. Xu, G. Chen, *Physica B*, 405 (2010) 803.
40. Y. Wang, Z.S. Feng, J.J. Chen, C. Zhang, X. Jin, J. Hu, *Solid State Commun.*, 152 (2012) 1577.
41. C.Y. OuYang, D.Y. Wang, S.Q. Shi, Z.X. Wang, H. Li, X.J. Huang, L.Q. Chen, *Chinese Phys. Lett.*, 23 (2006) 61.
42. G. Henkelman, H. Jo´nsson, *J. Chem. Phys.*, 113 (2000) 9978.
43. A. Urban, D.H. Seo, G. Ceder, *npj Comput. Mater.*, 2 (2016) 16002.
44. R. Car, M. Parrinello, *Phys. Rev. Lett.*, 55 (1985) 2471.
45. G. Xu, K. Zhong, J.M. Zhang, Z. Huang, *J. Appl. Phys.*, 116, (2014) 063703.
46. J. Yang, J. S. Tse, *J. Phys. Chem. A*, 115 (2011) 13045.
47. Y. Gao, K. Xiong, H.D. Zhang, B. Zhu, *ACS Omega*, 6, (2021) 14122.
48. F. Jiang, K. Qu, M. Wang, J. Chen, Y. Liu, H. Xu, Y. Huang, J. Li, P. Gao, J. Zheng, M. Chen and

 X. Li, *Sustain. Energ. Fuels*, 4 (2020) 2741.
49. C. Y. Ouyang, S. Q. Shi, Z. X. Wang, H. Li, X. J. Huang, L. Q. Chen, *Journal of Physics: Condens. Matter*, 16 (2004) 2265.
50. M. Wagemaker, B. L. Ellis, D. Lu¨tzenkirchen-Hecht, F. M. Mulder, L. F. Nazar, *Chem. Mater.*, 20 (2008) 6313.
51. T. Maxisch, G. Ceder, *Phys. Rev. B*, 73 (2006) 174112.
52. D.X. Zhang, J. Wang, K.Z. Dong, A. Hao, *Comp. Mater. Sci.*, 155 (2018) 410.
53. Y. Xie, H.T. Yu, T.F. Yi, Y.R. Zhu, *ACS Appl. Mater. Inter.*, 6 (2014) 4033.
54. S. L. Shang, Y. Wang, Z. G. Mei, X. D. Hui, Z. K. Liu, *J. Mater. Chem.*, 22 (2012) 1142